3D inversion of borehole to surface electromagnetic data in a multiple reservoirs survey

Alberto F. Marsala, Saudi Aramco, Michael S. Zhdanov, TechnoImaging and University of Utah, Masashi Endo and Noel Black, TechnoImaging*

Summary

There is a growing interest in developing innovative geophysical methods for monitoring hydrocarbon reservoirs. One emerging technique is based on using the borehole electric current transmitter and a grid of surface electric field receivers for detailed mapping of the subsurface resistivity of oil- and gas-producing fields. This method is often called Borehole to Surface Electromagnetic (BSEM) surveying. We introduce a rigorous method for 3D inversion of BSEM data based on the integral equation approach and adaptive regularization. We have applied our developed method to 3D inversion of a field BSEM dataset collected in a giant oilfield in Saudi Arabia. It was demonstrated that 3D inversion of the BSEM data can be effectively used for mapping and monitoring fluid distribution inside a reservoirs and imaging the oil-water contact.

Introduction

Over the last decade, there has been renewed interest in application of electromagnetic (EM) methods for oil and gas exploration and production monitoring. The most successful applications were related to marine EM and cross-well EM methods. One of the main challenges in application of the EM methods for reservoir monitoring is related to the fact that the target reservoir is relatively thin and deep. Considering the diffusive nature of EM fields, it is difficult to accurately resolve movement of fluids at depth based on surface observations only. One possibility to overcome this limitation of the surface data acquisition system is to place the source of the EM field into one borehole, closer to the reservoir, while keeping the receivers at the surface, on the ground. This approach is implemented in the borehole to surface EM (BSEM) method that consists of a borehole-deployed transmitter, and a surface-based array of receivers. BSEM technology was conceived in the former Soviet Union and fine-tuned by the Chinese Bureau of Geophysical Prospecting (BGP), (He et al., 2005, 2010). Saudi Aramco recently deployed the first BSEM pilot test outside of China. Marsala et al. (2011 a, b) have demonstrated successful applications of the BSEM method to identify the oil-water contact in the water-injection zone of carbonate reservoirs. We have developed a novel method of rigorous 3D inversion of the BSEM data. The paper presents the results of the application of developed 3D inversion method to the interpretation of BSEM field data collected over a major oil field in the northeastern Saudi Arabia.

Borehole-to-surface electromagnetic (BSEM) method

Figure 1 shows a typical BSEM survey configuration. In the framework of this method, the electric field is excited by vertical electric dipole transmitters, formed by a pair of electrodes, one located on the surface (electrode A0) and another one located at some depth in the borehole (electrodes A1 or A2), typically above and below a reservoir layer under investigation. The horizontal ($\mathrm{E_x}$ and $\mathrm{E_y}$) and/or the radial, $\mathrm{E_r}$, components of the electric field are measured on the surface of the Earth. The frequency of the electric field in BSEM varies typically within the range from 0.1 Hz up to 10 Hz. We denote by $\mathrm{E_{r1}}$ and $\mathrm{E_{r2}}$ the radial components of the field generated by electric dipole sources A0-A1 and A0-A2, respectively. We can then calculate a difference signal, $\Delta\mathrm{E} = \mathrm{E_{r2}} - \mathrm{E_{r1}}$, which represents the response of the target reservoir. Note that, one of the major difficulties with the EM measurements is the effect of the near-surface inhomogeneities caused by many near-surface artificial structures, such as boreholes with metal casing, near- surface infrastructure, pipelines, power lines, etc... The advantage of using a difference field, $\Delta\mathrm{E}$, for analysis and inversion of the BSEM data is based on the fact that the effect of near-surface geoelectrical inhomogeneities is significantly reduced in the difference field.

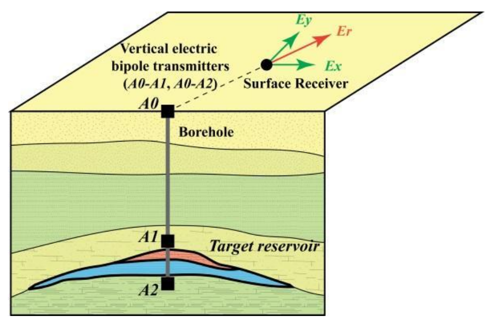

Figure 1: Sketch of a typical BSEM survey configuration.

Integral equation method in 3D inversion of BSEM data

The electric field recorded by the receivers can be represented as a sum of the background field, $\mathrm{E^b}$, generated in a horizontally layered background model, and an anomalous part, $\mathrm{E^a}$, related to the conductivity inhomogeneities $\Delta\sigma$ present in the reservoir layers:

$$\mathrm{E} = \mathrm{E^b} + \mathrm{E^a}.$$

DOI http://dx.doi.org/10.1190/segam2014-0455.1

The anomalous electric field is related to the electric current induced in the inhomogeneity, $\mathrm{j} = \Delta\sigma\mathrm{E}$, according to the following integral formula:

$$\mathrm{E}^{\mathrm{a}} = \iiint_{\mathrm{D}} \widehat{\mathrm{G}}_{\mathrm{E}} \cdot [\Delta\sigma\mathrm{E}]\mathrm{dv} = \mathrm{G}_{\mathrm{E}}[\Delta\sigma\mathrm{E}],$$

where $\widehat{\mathrm{G}}_{\mathrm{E}}$ is the electric Green's tensor defined for an unbounded conductive medium with the normal (horizontally layered) conductivity σ_{b}; G_{E} is corresponding Green's linear operator; and D represents a volume with the anomalous conductivity distribution $\sigma = \sigma_{\mathrm{b}} + \Delta\sigma$.

We use integral equation above to formulate both the forward and inverse problems of the BSEM method. This equation can be written in short form:

$$\mathrm{d} = \mathrm{A}(\Delta\sigma)\,,$$

where A is a forward modeling operator, d stands for the observed data, and $\Delta\sigma$ is a vector formed by the anomalous conductivities within the target domain. The inversion is based on minimization of the Tikhonov parametric functional P^{α}, with the corresponding stabilizing functional (Tikhonov and Arsenin, 1977):

$$\mathrm{P}^{\alpha}(\Delta\sigma) = \|\mathrm{W}_{\mathrm{d}}(\mathrm{A}(\Delta\sigma) - \mathrm{d})\|^{2}_{\mathrm{L}_2} + \alpha s(\Delta\sigma),$$

where W_{d} is the data-weighting matrix, and α is a regularization parameter.

There are several choices for the stabilizing functional (Zhdanov, 2002). The most common approach to the minimization of the parametric functional P^{α} is based on using gradient-type methods. We use the reweighted regularized conjugate gradient (RRCG) method introduced by Zhdanov (2002).

Case study

A world first innovative electromagnetic BSEM survey in an oil well completed with multiple casings has been acquired in a giant mature oil field located in the North of Eastern Province of Saudi Arabia (Marsala et al., 2013). The objective was to deploy a single BSEM survey to map the oil / water distributions in two separate reservoirs. The production from this field has been primarily from two fractured carbonate reservoirs, Upper and Lower, which are separated by a 500ft thick, non-reservoir limestone formation. The Upper reservoir is prolific throughout the whole field and its high rate producers have been responsible for the majority of the historic field production. The Upper reservoir performance, including water flood fronts, has been very predictable, which have made it easy to identify well targets and plan successful new development wells, sidetracks and other well remedial action based solely on well data like production performance, inflow profiles and saturation logs. The Lower reservoir is oil bearing only in the southern part of the field. This reservoir has low matrix permeability with well productivities and inflow profiles controlled mainly by a complex fracture system. A comprehensive Lower reservoir development drilling program is currently ongoing to augment the Upper reservoir production. Due to the complex fracture system, the Lower reservoir development drilling program has been prone to unpredictable well fluid saturation results.

The reservoir pressure data from the early production period confirmed communication between the two reservoirs through several large scale fractures crossing the non-permeable zone. In the Lower reservoir, well log observations show a variable oil/water distribution.

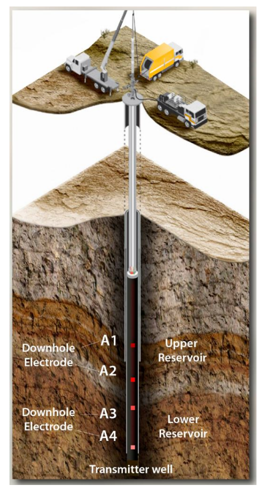

Figure 2: The downhole transmitting electrode of a vertical electric dipole is deployed below and above each reservoir layer under investigation.

No direct measurements of fluid saturations are available in the inter-well areas. This data gap is now intended filled by electromagnetic surveys. The business impact is to increase recovery by maximizing sweep efficiency and optimize well placements.

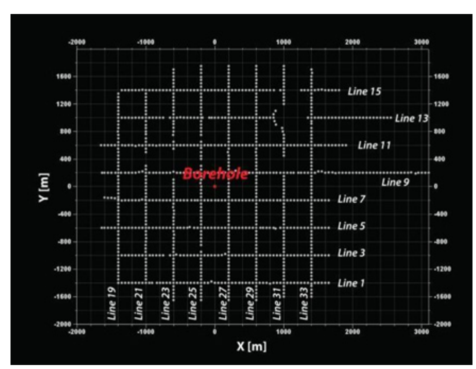

Figure 3: locations of the transmitter wellhead (Borehole) and the receivers' lines used for the 3D inversion of BSEM data.

DOI http://dx.doi.org/10.1190/segam2014-0455.1

EM signals were transmitted at multiple frequencies from four source locations placed in the single transmitting well across both reservoirs (Figure 2) and received by more than 1000 surface stations, located in a grid at distances up to 3 kilometers away from the transmitting wellhead.

BSEM data were collected along sixteen observation lines, shown in Figure 3. The data were measured at 63 frequencies from 0.02 to 10 Hz. Based on the analysis of the noise level in the observed BSEM data (difference signals) and numerical experiments with the inversion of these data, three frequencies (0.1, 0.3, and 1.1029 Hz) were selected as optimal ones for the final 3D inversion.

Figure 4 presents the profiles of the observed radial electric field data as difference BSEM signals above and below Upper and Lower reservoirs; i.e. A2-A1 (Upper reservoir) and A4-A3 (Lower reservoir), respectively, for three selected frequencies (0.1, 0.3, and 1.1029 Hz).

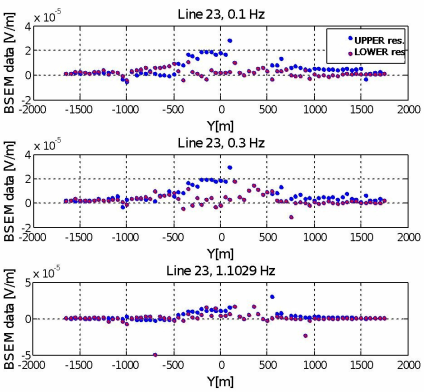

Figure 4: Profiles of observed electric field data as a difference of BSEM signals above and below the Upper reservoir (A2-A1, blue), and above and below the Lower reservoir (A4-A3, purple). On the abscissa the distance from the transmitting wellhead location.

The effect of near-surface geoelectrical inhomogeneities was significantly reduced in the difference electric field, due to remote location of the current electrodes in the borehole. We have also applied regularization in our 3D inversion method, which suppresses the noise in the data, while preserving useful information about the resistivity distribution within the target reservoirs.

We have run simultaneous inversion for the data collected along all the sixteen survey lines for three optimal frequencies, identified above. The final inversion model of the recovered resistivity in the survey area was produced within the volume of 5 km x 4 km x 2.3 km in the x, y, and z directions, respectively, discretized into 10m x 10m x 2m. The inversion software is fully parallelized, and all the inversions were run on a PC cluster. Figure 5 shows the porosity distribution on the field section structure, comprising upper and lower reservoirs; surface receivers grid and well trajectory are visible, along with the entire cube of the 3D resistivity inversion.

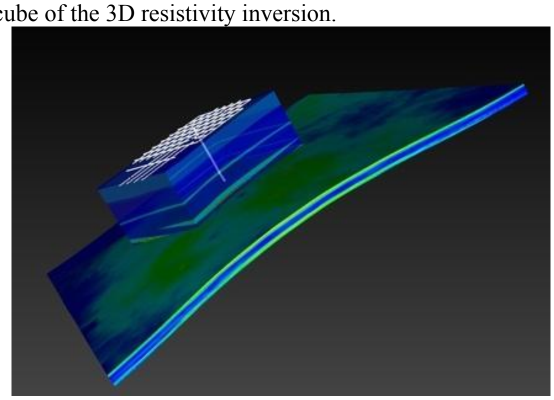

Figure 5: Porosity map of the upper and lower reservoir structure, along with the entire 3D inversion cube.

Detailed perspective of the 3D resistivity inversion cube is presented in Figure 6. The resistivity distributions within the two reservoir layers are very visible at the base of the cube, nestled between very resistive cap rocks (anhydrite) and basement layers.

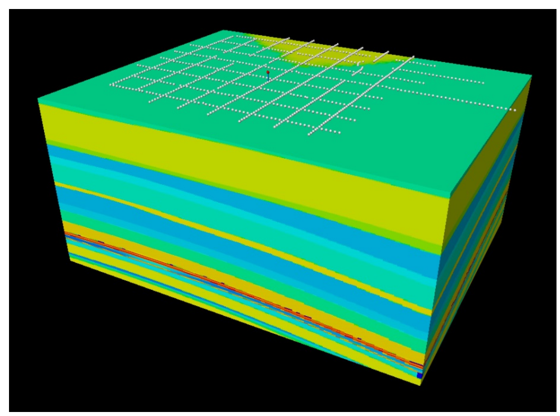

Figure 6: 3D resistivity inversion cube.

Upper reservoir

We have performed 3D inversion of the BSEM data for the resistivity distribution of the Upper reservoir. Figure 7 shows examples of profiles of the observed BSEM data, which were processed for the inversion, and predicted BSEM data as outputs of the inversion, along Line 31. One can see that the predicted data fit the observed data reasonably well. Figure 8 shows the recovered 3D resistivity distribution of the Upper reservoir, with surrounding background geoelectrical structure. Note that the background structure was defined using lithological surfaces and well-log data available in the survey area. It can be observed the resistive (reddish color) and conductive (bluish color) zones within the volume, corresponding to

DOI http://dx.doi.org/10.1190/segam2014-0455.1

the Upper reservoir, located within a resistive background geoelectrical structure.

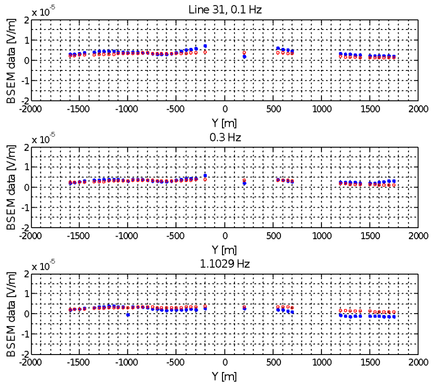

Figure7: Profiles of the observed (processed for inversion, blue dots) and predicted (red circles) BSEM data along Line 31 for frequencies of 0.1 (upper), 0.3 (middle) and 1.1029 (bottom) Hz.

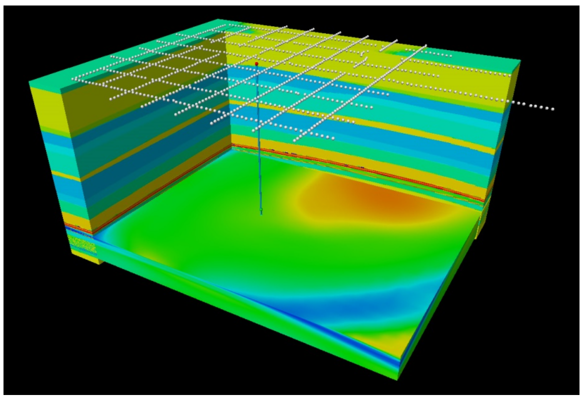

Figure 8: The recovered 3D resistivity distribution of the Upper reservoir with the background geoelectrical structure.

Lower reservoir

Similarly we have performed 3D inversion of the BSEM data for the resistivity distribution of the Lower reservoir. Figure 9 shows examples of profiles of the observed BSEM data and predicted BSEM data as outputs of the inversion, along Line 1. Figure 10 shows the recovered 3D resistivity distribution of the Lower reservoir, with surrounding background geoelectrical structure. One can observe the resistive (reddish color) and conductive (bluish color) zones of the Lower reservoir located within a resistive background geoelectrical structure.

Conclusions

We have developed rigorous algorithm and parallelized software for 3D inversion of borehole to surface electromagnetic (BSEM) data. We have applied our method for 3D inversion of the field BSEM data collected in a giant oilfield in northeastern Saudi Arabia.

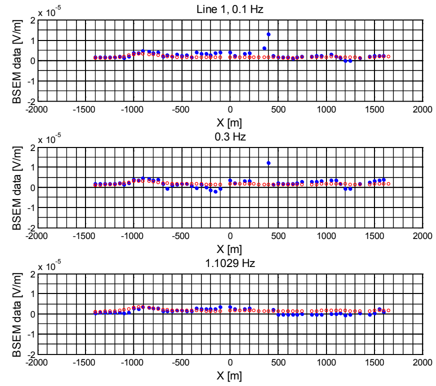

Figure 9: Profiles of the observed (blue dots) and predicted (red circles) BSEM data along Line 1 for frequencies of 0.1 (upper), 0.3 (middle) and 1.1029 (bottom) Hz, respectively.

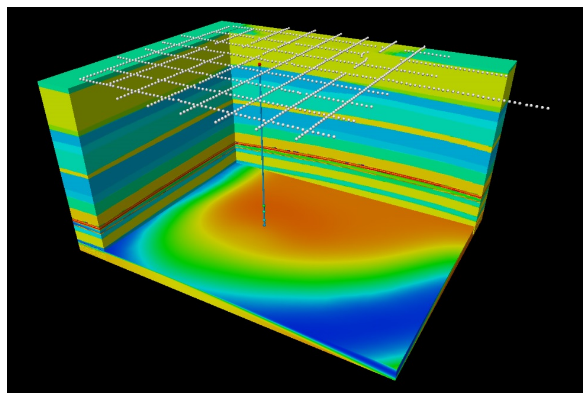

Figure 10: The recovered 3D resistivity distribution of the Lower reservoir with the background geoelectrical structure.

Accurate fluid distribution analysis in the Upper and Lower reservoirs is ongoing, integrating the results of 3D BSEM resistivity and chargeability data, with well logs, geological, static and dynamic reservoir simulation information. It was demonstrated that BSEM survey can be used for monitoring oil reservoirs, especially for the location of the oil-water contact, due to the significant contrast of the resistivities between oil and water saturated layers. Future research will be aimed at the analysis of both electric and magnetic components of the EM field generated by the borehole source, and at examining the possible induced polarization (IP) effect in the observed data.

Acknowledgements

Authors acknowledge Saudi Aramco and TechnoImaging for the support to this project and the permission to publish.

DOI http://dx.doi.org/10.1190/segam2014-0455.1

http://dx.doi.org/10.1190/segam2014-0455.1

EDITED REFERENCES

Note: This reference list is a copy-edited version of the reference list submitted by the author. Reference lists for the 2014 SEG Technical Program Expanded Abstracts have been copy edited so that references provided with the online metadata for each paper will achieve a high degree of linking to cited sources that appear on the Web.

REFERENCES

He, Z., W. Hu, and W. Dong, 2010, Petroleum electromagnetic prospecting advances and case studies in China: Surveys in Geophysics, **31**, no. 2, 207–224, http://dx.doi.org/10.1007/s10712-009-9093-z.

He, Z., X. Liu, W. Qiu, and H. Zhou, 2005, Mapping reservoir boundary by borehole surface TFEM: Two case studies: The Leading Edge, **24**, 896–900, http://dx.doi.org/10.1190/1.2056379.

Marsala, A. F., M. H. Al-Buali, Z. A. Ali, S. M. Ma, Z. He, T. Biyan, G. Zhao, and T. He, 2011a, First borehole to surface electromagnetic survey in KSA: Reservoir mapping and monitoring at a new scale: SPE Annual Technical Conference and Exhibition, SPE-146348.

Marsala, A. F., M. H. Al-Buali, Z. A. Ali, S. M. Ma, Z. He, T. Biyan, G. Zhao, and T. He, 2011b, First pilot of borehole to surface electromagnetic in Saudi Arabia: A new technology to enhance reservoir mapping and monitoring: 73rd Annual International Conference and Exhibition, EAGE, Extended Abstracts, I005.

Marsala, A. F., S. Lyngra, D. Widjaja, A. Laota, N. Al-Otaibi, Z. He, G. Zhao, J. Xu, and C. Yang, 2013, Fluid distribution inter-well mapping in multiple reservoirs by innovative borehole to surface electromagnetic: Survey design and field acquisition: International Petroleum Technology Conference, IPTC-17045.

Tikhonov, A. N., and V. Y. Arsenin, 1977, Solution of ill-posed problems: V. H. Winston and Sons.

Zhdanov, M. S., 2002, Geophysical inverse theory and regularization problems: Elsevier Science Publishing Company, Inc.